

Article

Prediction of Compressive Strength of Rice Husk Ash Concrete through Different Machine Learning Processes

Ammar Iqtidar ^{1,*}, Niaz Bahadur Khan ², Sardar Kashif-ur-Rehman ¹, Muhammad Faisal Javed ¹, Fahid Aslam ³, Rayed Alyousef ³, Hisham Alabduljabbar ³ and Amir Mosavi ^{4,5,*}

- ¹ Department of Civil Engineering, Abbottabad Campus, COMSATS University Islamabad, Abbottabad 22060, Pakistan; skashif@cuiatd.edu.pk (S.K.-u.-R.); arbabfaisal@cuiatd.edu.pk (M.F.J.)
² School of Mechanical & Manufacturing Engineering, National University of Sciences & Technology, Islamabad 44000, Pakistan; niaz.bahadur@smme.nust.edu.pk
³ Department of Civil Engineering, College of Engineering in Al-Kharj, Prince Sattam Bin Abdulaziz University, Al-Kharj 11942, Saudi Arabia; f.aslam@psau.edu.sa (F.A.); r.alyousef@psau.edu.sa (R.A.); h.alabduljabbar@psau.edu.sa (H.A.)
⁴ Faculty of Civil Engineering, Technische Universitat Dresden, 01069 Dresden, Germany
⁵ John von Neumann Faculty of Informatics, Obuda University, 1034 Budapest, Hungary
* Correspondence: FA16-BCV-016@cuiatd.edu.pk (A.I.); amir.mosavi@mailbox.tu-dresden.de (A.M.)



Citation: Iqtidar, A.; Bahadur Khan, N.; Kashif-ur-Rehman, S.; Faisal Javed, M.; Aslam, F.; Alyousef, R.; Alabduljabbar, H.; Mosavi, A. Prediction of Compressive Strength of Rice Husk Ash Concrete through Different Machine Learning Processes. *Crystals* **2021**, *11*, 352. <https://doi.org/10.3390/cryst11040352>

Academic Editors: Shujun Zhang and Yifeng Ling

Received: 13 February 2021

Accepted: 22 March 2021

Published: 29 March 2021

Publisher's Note: MDPI stays neutral with regard to jurisdictional claims in published maps and institutional affiliations.



Copyright: © 2021 by the authors. Licensee MDPI, Basel, Switzerland. This article is an open access article distributed under the terms and conditions of the Creative Commons Attribution (CC BY) license (<https://creativecommons.org/licenses/by/4.0/>).

Abstract: Cement is among the major contributors to the global carbon dioxide emissions. Thus, sustainable alternatives to the conventional cement are essential for producing greener concrete structures. Rice husk ash has shown promising characteristics to be a sustainable option for further research and investigation. Since the experimental work required for assessing its properties is both time consuming and complex, machine learning can be used to successfully predict the properties of concrete containing rice husk ash. A total of 192 data points are used in this study to assess the compressive strength of rice husk ash blended concrete. Input parameters include age, amount of cement, rice husk ash, super plasticizer, water, and aggregates. Four soft computing and machine learning methods, i.e., artificial neural networks (ANN), adaptive neuro-fuzzy inference system (ANFIS), multiple nonlinear regression (NLR), and linear regression are employed in this research. Sensitivity analysis, parametric analysis, and correlation factor (R^2) are used to evaluate the obtained results. The ANN and ANFIS outperformed other methods.

Keywords: rice husk ash; sustainable concrete; artificial neural networks; multiple linear regression; eco-friendly concrete; green concrete; sustainable development; artificial intelligence; data science; machine learning

1. Introduction

The world is making progress by leaps and bounds. New technologies and innovations are being introduced every day in every field. These advancements have altered the course of human history. One of the main aspects that has played a crucial role in shaping modern human civilization is infrastructure. From caves, mankind has started to live in strong and pleasing dwellings made by their own creative and innovative minds. Still, today infrastructure is considered to be the main element for progress in any country. The construction material that is used in abundance throughout the world for the construction of infrastructure is cement. However, along with the advantages of cement there are also certain adverse effects. Cement is said to be responsible for seven percent of the total carbon dioxide emissions worldwide [1]. It produces carbon dioxide while reacting when water is added to it. Secondly, a high temperature is required during the production of cement [2]. This high temperature is achieved by burning fossil fuels which increase the carbon footprint of cement. Our planet earth is suffering from problems of grave danger. Environmental deterioration and global warming are some of these alarming issues. If not

controlled in due time, these problems will push the earth to the brink of extinction. One of the major causes of environmental degradation and global warming is said to be the emission of carbon dioxide from different products and processes [3,4]. Since cement is a crucial contributor to the total carbon dioxide emissions of the world, the importance of infrastructure cannot be undermined. It must be replaced with some other material that has a smaller carbon footprint as well as possessing the same or better properties than cement.

The materials that replicate the properties of ordinary Portland cement (OPC) are known as secondary cementitious materials (SCMs). They have smaller carbon dioxide emission rates [5]. SCMs are generally waste materials and byproducts of different industries. These materials become sources of various types of pollution if not discarded or utilized properly. SCMs can be used in different proportions and combinations to replicate the desired properties of OPC. Some of the SCMs are fly ash (FA), corn cob ash (CCA), sugarcane bagasse ash (SCBA), rice husk ash (RHA), ground granulated blast furnace slag (GGBFS), etc [6–9]. RHA is one of the SCMs obtained from the agricultural waste of rice crop. Rice grains are covered in rice husks (RH) which are used as a fuel to boil paddy in rice mills. RHA is obtained after utilizing rice husks as fuel. It contains more than 90 percent silica and can be used successfully as an SCM to synthesize concrete [10]. An illustration of the chemical composition of RHA is shown in Figure 1 [11]. Ameri et al. [12] conducted a research on concrete containing RHA. It was found that concrete containing RHA showed a vigorous increase in early compressive strength. However, by increasing the RHA content by more than 15 percent, the compressive strength was decreased. This is attributed to the excess amount of silica present in RHA which remains unreacted. The compressive strength of concrete with RHA as an SCM was 9, 12, 13, and 16 percent higher than that of control mix. Similarly, Chao Lung et al. [13] incorporated RHA in concrete and concluded that concrete containing RHA showed a strength 1.2 to 1.5 times greater than that of the control mix. Chindaprasirt et al. [14] tested the concrete containing RHA for sulphate attack resistance and reported that concrete containing RHA proved to be highly effective against sulphate attack. It was reported by Thomas et al. [15] in a review paper that concrete containing RHA has a dense microstructure, so it can be used to reduce the water absorption of concrete by up to 30 percent. Rattanachu et al. [16] conducted research in which grounded RHA was used with steel reinforcements. It was observed that the use of RHA in the presence of steel resisted the corrosion of steel due to the fine structure of RHA. Thus, several studies have been made on environmental impact of RHA. They are reported in Table 1:

Table 1. Environmental impact of rice husk ash (RHA).

Material in Which RHA Is Used	Results	Reference
Concrete	Utilization of RHA results in reduction of global warming potential (GWP)	[17]
Mortar	Use of RHA results in reduction of harmful environmental impacts	[18]
Concrete	RHA aids in reducing carbon footprint of concrete	[19]
Concrete blocks	Utilization of RHA shows positive environmental results	[20]

Hence, RHA can be utilized successfully as a cementitious material. RHA does not produce excessive amount of carbon dioxide. It can be used as a structural concrete. Not only does it contribute towards the strength of the concrete but also towards the long term durability properties of concrete [21].

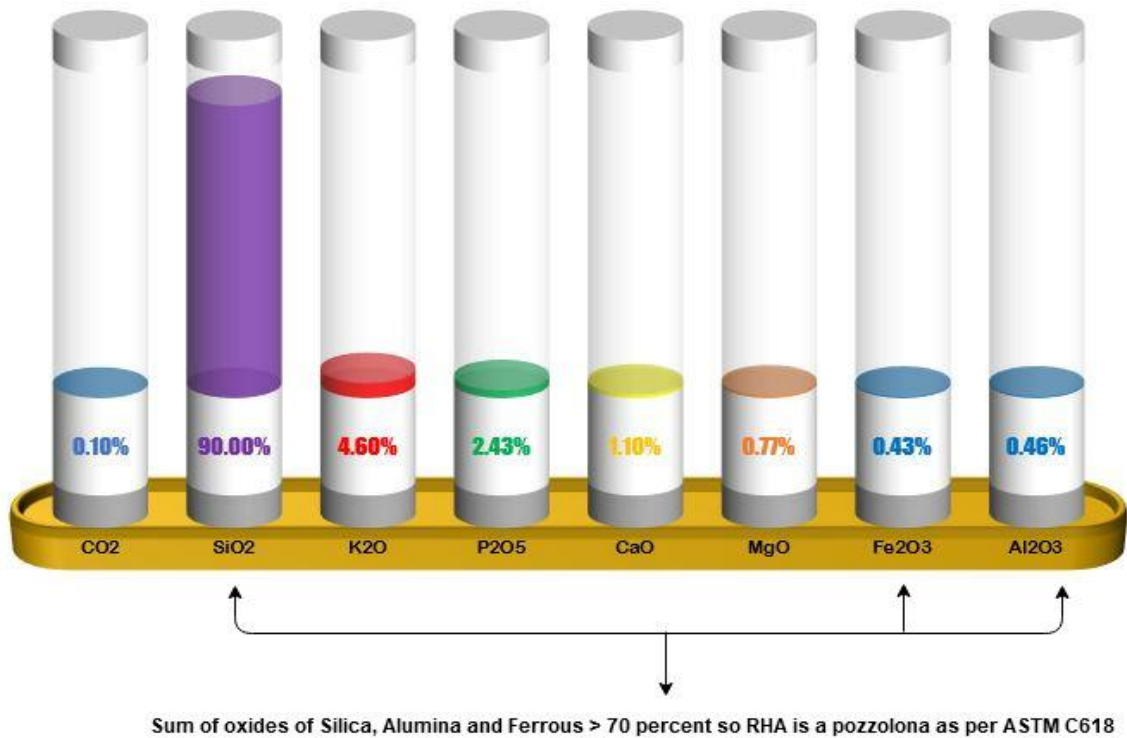


Figure 1. Chemical composition of RHA.

The rate of environmental deterioration does not allow one to spend an extensive amount of time on research and development of RHA blended concrete (RBC). Consequently, extensive lab works cannot be carried out on RBC. Along with that there is always an uncertainty regarding the mix design of RBC. This is due to the hygroscopic nature of RHA. Therefore, to predict the properties of different SCMs, artificial intelligence (AI) is being used throughout the globe. AI is used by different researchers to assess and predict the strength of concrete mixes. Table 2 lists the different previous studies conducted on SCMs to predict different properties. Different techniques such as artificial neural networks (ANN), LR, adaptive neuro-fuzzy inference system (ANFIS), and MNLr are used to successfully model and predict different properties of materials [22,23].

As AI research depends on mathematical modelling and parameters, it is a complex programming work and needs great optimization and care. Therefore, four programming techniques are being used to predict the compressive strength of RHA-based concrete in this research. These techniques are ANFIS, ANN, MNLr, and LR. To achieve the targeted accuracy and to cater the complexity of programming these four techniques will be compared with each other. A vast database of peer reviewed literature is used to model the prediction of compressive strength.

Table 2. Some recent studies using AI.

Material Used	No. of Data Points	Property Predicted	Modelling Technique Used	Reference
SCBA	65	Compressive strength	GEP, Multiple Linear Regression (MLR), Multiple Nonlinear Regression (MNLN)	[22]
Silica fume (SF) and zeolite	18	Compressive Strength	ANN	[23]
Recycled concrete aggregate	17	Compressive strength	ANN, Response Surface Methodology (RSM)	[24]
Recycled rubber concrete	72	Compressive strength	ANN, MNLN, ANFIS, Support vector machine (SVM)	[25]
Cellular concrete	99	Compressive strength	Backpropagation Neural Network (BPNN)	[26]
Fly ash (FA) and blast furnace slag (BFS)	135	Compressive strength	ANN	[27]
Foamed concrete	91	Compressive strength	Extreme Learning Machine (ELM)	[28]
Recycled aggregates	74	Compressive strength	ANN Convolutional Neural Network	[29]
Rubberized concrete	112	Compressive strength	ANN	[30]
Steel fiber added lightweight concrete	126	Compressive strength	ANN	[31]
Fiber reinforced polymer concrete (FRP)	98	Shear strength	ANN	[32]
FRP	84	Shear strength	ANN	[33]
High strength concrete (HSC)	187	Compressive strength	ANN	[34]

2. Data Collection

To predict the compressive strength (CS) of RHA, mathematical models are developed using a dataset of 192 data points from the vast literature review and existing studies on machine learning [12,13,35–39]. These data were collected through google Scopus. The constituents of concrete include RHA, OPC, aggregates, super plasticizer (SP), and water. The type of cement and curing methodology used in all the mixes is same. The CS of cubic specimens is converted into CS of cylinders by using 0.8 as a factor (as per BS 1881: Part 120:1983). The only output parameter in this study is compressive strength. The input parameters consist of main variables such as percentage of SP, curing age (CA), quantity of water used (W), amount of OPC (OPCP), quantity of aggregates (AGG), and amount of RHA (RHAP). Moreover, the description of collected data and its statistics are given in Table 3.

Table 3. Statistical analysis of input data.

Parameters	Mean	Standard Deviation	Kurtosis	Skewness	Minimum	Maximum
Input parameters						
Age (days)	34.57	33.52	−1.02	0.75	1	90
Plain cement (kg/m ³)	409.02	105.47	3.66	1.55	249	783
RHA (kg/m ³)	62.33	41.55	0.07	0.44	0	171
Water (kg/m ³)	193.54	31.93	−0.74	−0.42	120	238
Super plasticizer (kg/m ³)	3.34	3.52	−0.82	0.69	0	11.25
Aggregates (kg/m ³)	1621.51	267.77	−0.27	−0.74	1040	1970
Response						
Experimental compressive strength (MPa)	48.14	17.54	0.75	0.83	16	104.1

3. Methodology

The methodology section provides a brief detail about the approaches being made to determine the CS of concrete mathematically as shown in Figure 2. First, the AI processes used in this research are explained. The results obtained from AI data processing techniques are assessed for validity by different statistical parameters.

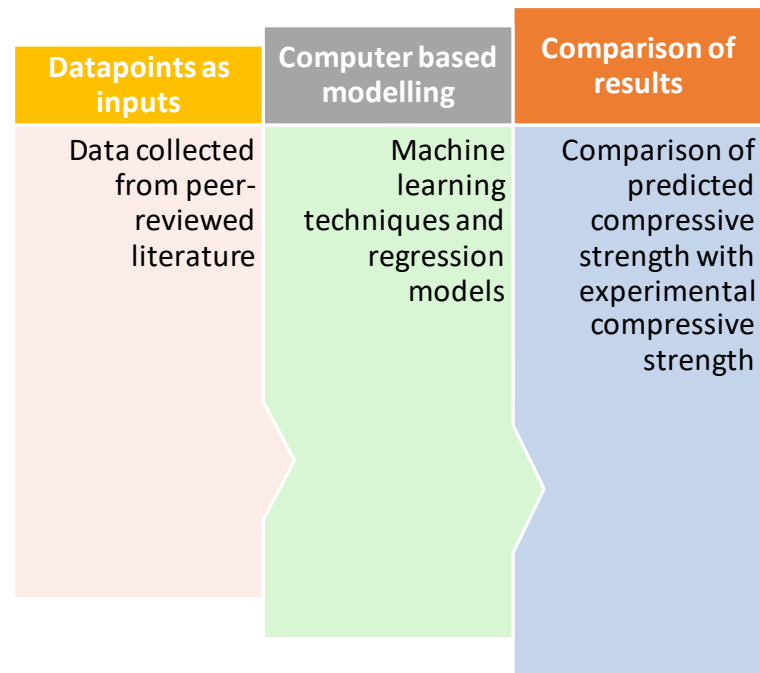


Figure 2. Adopted methodology for study.

3.1. Modeling Techniques

Machine learning-based modeling has been used in the past to predict the different mechanical properties of materials [40–42]. These types of modeling techniques can be utilized to develop models for prediction of a property of material. They do not need any knowledge of the rudimentary experimental processes. This section of paper provides a brief introduction of the predictive models used in this study. These models are as follow:

3.1.1. ANN

ANN is an artificial data analyzing technique. It is inspired by the learning capability of human brain. The most widely used type of ANN is feedforward back propagation (FFBP). As evident from Figure 3, an FFBP consists of at least three layers, namely, the input layer, hidden layer, and output layer. The nodes of these layers are connected in a proper sequence along with some weights. The input layer nodes do not perform any function on input data. Their function is to just receive the data from outside. It is a hidden layer where data are biased, weighted, and summed up. These processed data are then sent out to the output layers [43,44].

There are basically two types of FFBP, namely, single layer perceptron (SLP) and multiple layers perceptron (MLP). Both types of FFBP have their own advantages and disadvantages. Although the SLP is simple and easy to use, it cannot handle nonlinear relations. On the other hand, MLP are complex, but they can be applied to nonlinear relations.

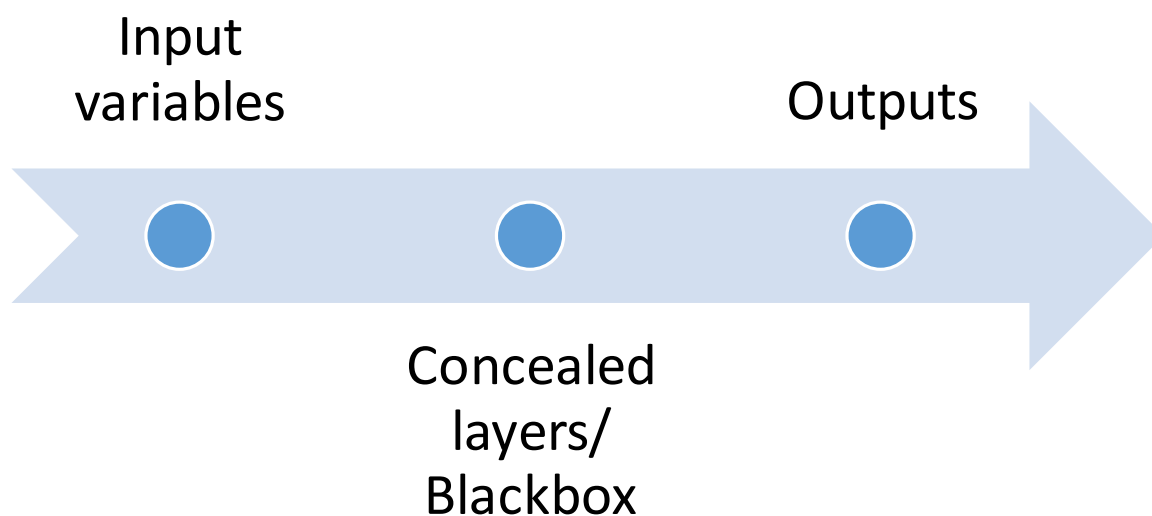


Figure 3. Illustration of ANN.

Mathematically, an MLP operates in following way:

Step 1: The inputs are summed and weighted as

$$s_j = \sum_{i=1}^n \omega_{ij} I_i + b_j \quad j = 1, 2, 3, \dots, h \tag{1}$$

where n = number of total inputs, I_i = current input number, ω_{ij} = weight between the previous layer, and the j th neuron and b are used to define the termination of process.

Step 2: This step includes an activation function. There are various types of activation functions such as sigmoid, ramp, and Gaussian functions. However, this research utilizes sigmoid function which is defined as

$$s_j = \frac{1}{1 + e^{-s_j}} \quad j = 1, 2, 3, \dots, h \tag{2}$$

Step 3: This represents the final outputs. The final outputs depend on the outputs calculated by hidden nodes. The final outcome can be expressed as

$$O_k = \sum_{j=1}^h (\omega_{jk} \cdot s_j) + b'_k, \quad k = 1, 2, \dots, m \tag{3}$$

$$O_k = \text{sigmoid}(O_k) = \frac{1}{(1 + e^{-O_k})}, \quad k = 1, 2, \dots, m \tag{4}$$

In above equation, ω_{jk} = weighted connection between k th output node to j th hidden node. Similarly, b'_k = bias output of k th output node.

In this research, 70 percent of the data points are selected randomly for the training of data, and 30 percent for validation.

3.1.2. ANFIS

ANFIS is a technique that utilizes the combined effect of artificial neural networks and fuzzy logic [45]. Figure 4 shows a brief illustration of the ANFIS technique. An artificial neural network is used to minimize the chances of error in the output data. Thus, the fuzzy logic is implied to demonstrate the expert knowledge [42]. Fuzzy logic rules are applied as if-then while mathematically programming for the desired input and output datasets. An ANFIS model consists of five layers normally. These are (1) fuzzification, (2) set of rules, (3) normalization, (4) defuzzification, (5) aggregation.

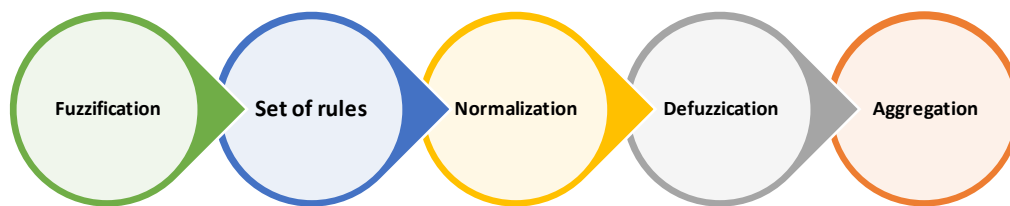


Figure 4. Illustration of adaptive neuro-fuzzy inference system (ANFIS).

Layer 1 is the fuzzification layer. It contains all the function members of the input variables. A Gaussian function is used in this layer to predict the outcome. Mathematically, it can be expressed as

$$\mu_{ui}(x) = \exp\left[-\frac{(x - a_i)^2}{2 \varepsilon_i^2}\right] \quad (5)$$

where a_i and ε_i are parameters of a function membership.

Layer 2 contains nodes which send the output by multiplying the input by certain weightages. This layer utilizes the fuzzy AND logic by using the equation listed below:

$$w_i = \mu_{ui}(x) \times \mu_{vi}(y) \quad (6)$$

Layer 3 has an aim to normalize the data. It normalizes the functions of membership. It calculates the ratios between different firing strength using the following expression:

$$\bar{w} = \frac{w_i}{\sum_i w_i} \quad (7)$$

Layer 4 is known as the defuzzification layer. It contains nodes that conclude the fuzzy logic rules. This layer contains square nodes, which can be expressed by following function:

$$\bar{w}_i f_i = w_i \times (m_i x + n_i y + r_i) \quad (8)$$

where m_i , n_i , and r_i are linear parameters.

Layer 5 has a function of aggregation. It sums up the previous layers and presents the final output mathematically as follows:

$$\sum_i \bar{w}_i f_i = \frac{\sum_i w_i f_i}{\sum_i w_i} \quad (9)$$

All the data points are used for the training of data.

Off the shelf functionality of MATLAB is used for ANN and ANFIS techniques in this research.

3.1.3. MNLR

MNLR is a technique which is used to model a random nonlinear relationship between the dependent and independent variables. The following equation represents the MNLR [41]:

$$Y = a + \beta_1 X_i + \beta_2 X_j + \beta_3 X_i^2 + \beta_4 X_j^2 + \dots + \beta_k X_i X_j \quad (10)$$

where a = intercept, β = slope or coefficient, K = number of observations. The above equation can make an estimate for the value of Y for each value of X .

3.1.4. LR

LR is a technique in which there is linear relationship between the dependent and independent variables. It can be represented mathematically as follows:

$$Y = a + \beta_1 X_1 + \beta_2 X_2 + \beta_3 X_3 + \dots + \beta_i X_i \quad (11)$$

The above equation can be utilized to find values of Y for each input value X .

In above equations of MNL and LR, “ Y ” stands for compressive strength of RHA. Similarly, the values of “ X ” represents inputs which are age, water content, RHA content, SP content, and the percentage of aggregates.

The models are developed in Microsoft Excel by authors for MNL and LR techniques using the above equations.

4. Results

A total of 192 data points are used for all the models and techniques. A total of 134 data points are used for training, and 58 data points for validation. The results of machine learning techniques and regression models are given in Appendix A.

4.1. ANN

Parametric adjustments are made before running the proposed ANN model. These parameters include number of hidden layers, total number of neurons per hidden layer, training function for neural networks, epochs, and maximum number of iterations. These parameters are determined through the hit and trial method in this research. The details of the parametric adjustment are given in Table 4.

Table 4. Parametric adjustment of the developed model.

Parameters	Description
Total number of hidden layers	2
Maximum number of neurons per hidden layer	10
Training function	Levenberg–Marquardt
Epochs	3
Training completed at epoch	2

MATLAB was used to predict the compressive strength of RBC through ANN. ANN gave the results which were closest to the experimental results. The same can be verified through the statistical parameters of ANN.

It is noteworthy that the correlation factor for ANN predicted CS ($R^2 = 0.98$) is quite high. The prediction result for ANN is plotted in Figure 5.

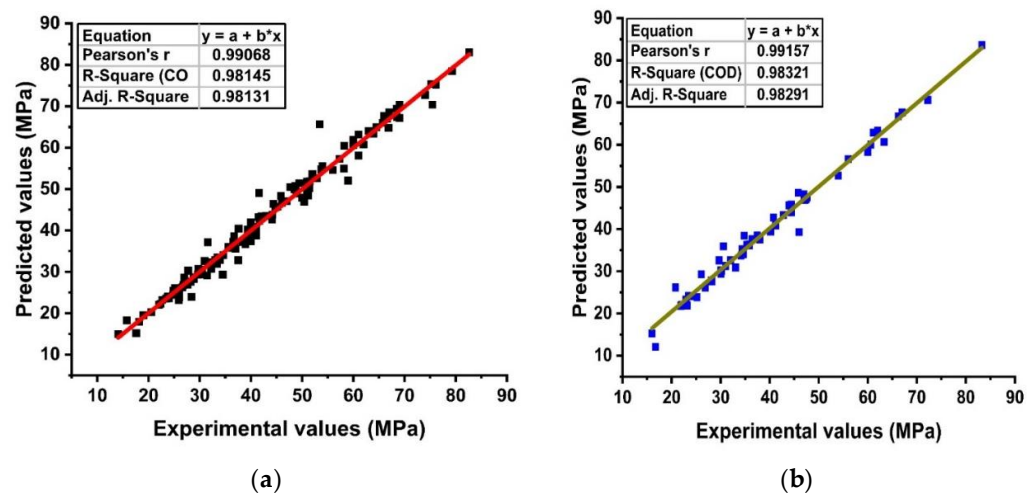
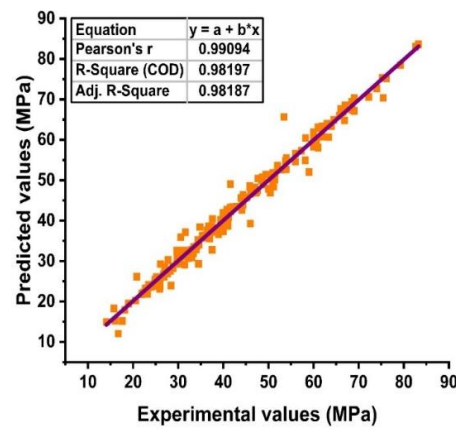


Figure 5. Cont.



(c)

Figure 5. ANN (a) training, (b) validation, (c) testing.

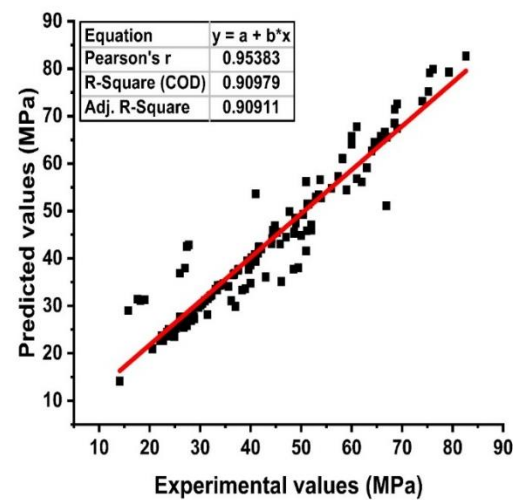
4.2. ANFIS

Similarly, before training the data on ANFIS, parametric adjustments were made. These included total number of epochs and function used for the activation of ANFIS. The parametric adjustments for ANFIS are given in Table 5.

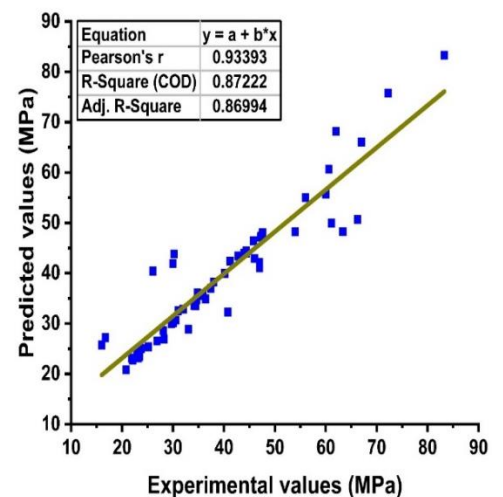
Table 5. Parametric adjustments for ANFIS.

Parameters	Description
Training function	trimf
Epochs	6
Training completed at epoch	2

MATLAB is used for ANFIS. The correlation factor for ANFIS predicted CS ($R^2 = 0.89$) is also quite high. Figure 6 shows that the predicted results are quite close to the experimental values.



(a)



(b)

Figure 6. Cont.

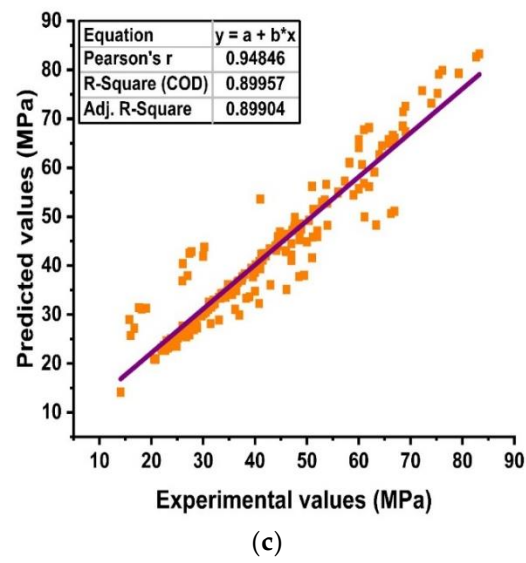
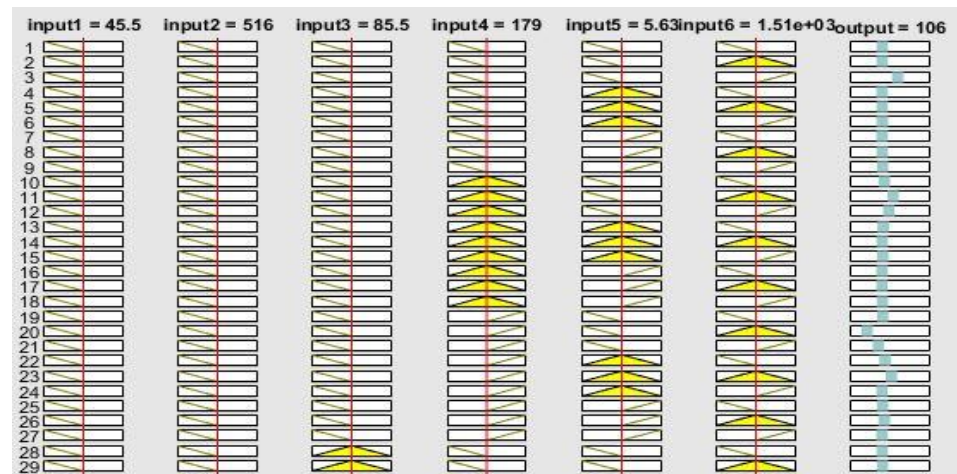
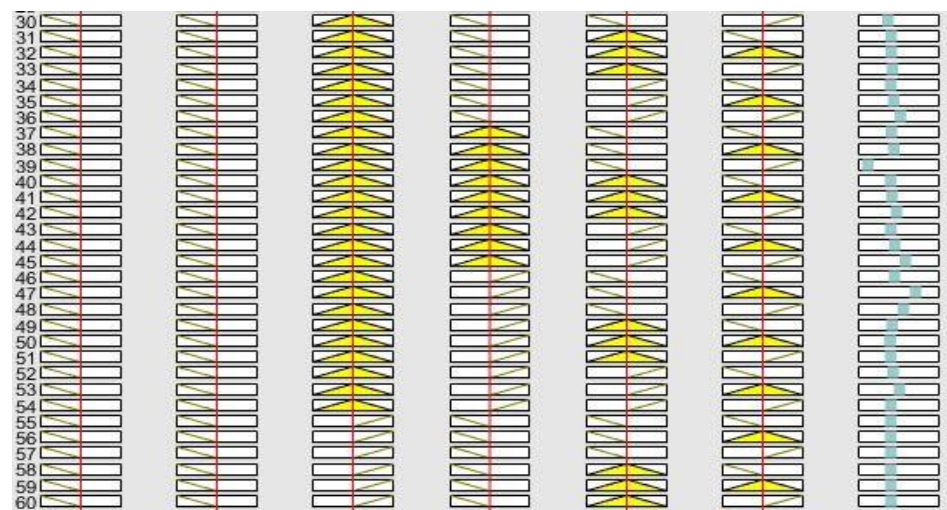


Figure 6. ANFIS (a) training, (b) validation, (c) testing.

Figure 7 shows the rules assigned to ANFIS for the optimum outcome.



(a)



(b)

Figure 7. Cont.

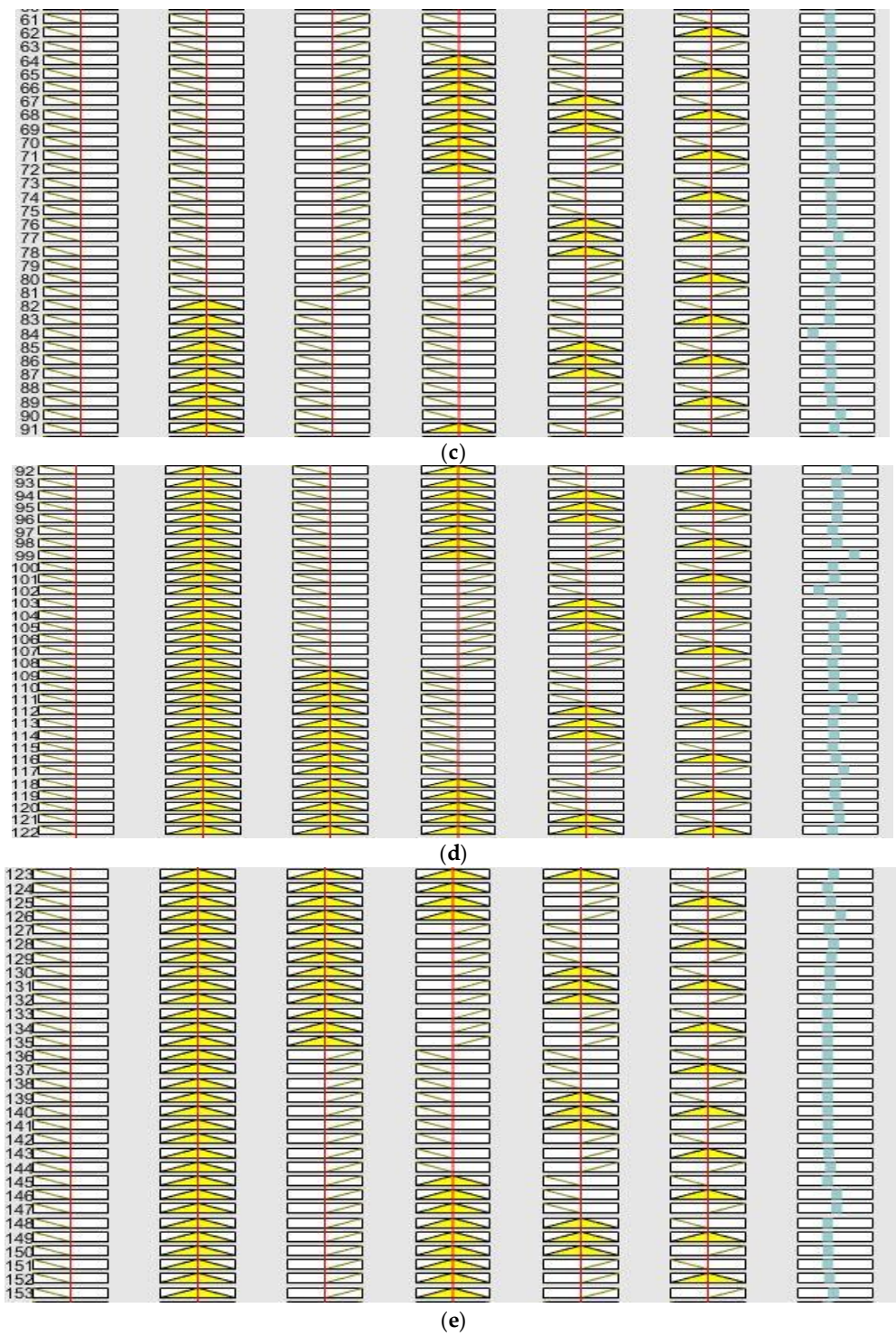


Figure 7. Cont.

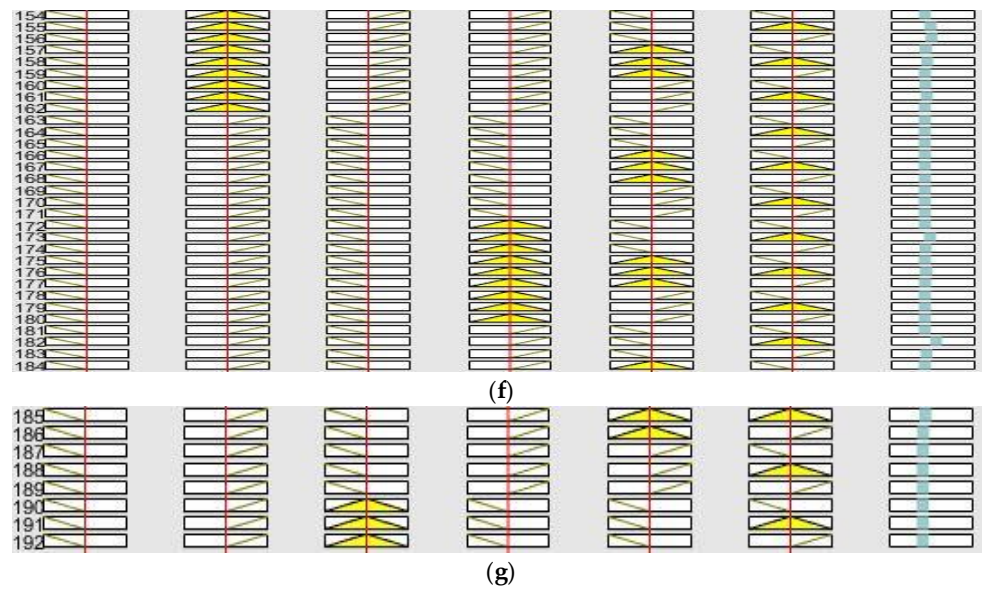


Figure 7. ANFIS modeling rules. (a) 1–29, (b) 30–60, (c) 61–91, (d) 92–122, (e) 123–153, (f) 154–184, (g) 185–192.

4.3. MNLN

The results predicted by MNLN were not close to the experimental results. The correlation factor for MNLN predicted CS ($R^2 = 0.70$) confirms the same. The correlation factor for training and validation is 0.75 and 0.69, respectively. The same can be confirmed by the dispersion of points in Figure 8 below.

4.4. LR 40

LR gave the results which were far away from the experimental results. A weak correlation ($R^2 = 0.63$) existed between the experimental and predicted results. The correlation factor for LR training and LR validation is 0.64 and 0.62, respectively. It can be seen in Figure 9 below that points are dispersed.

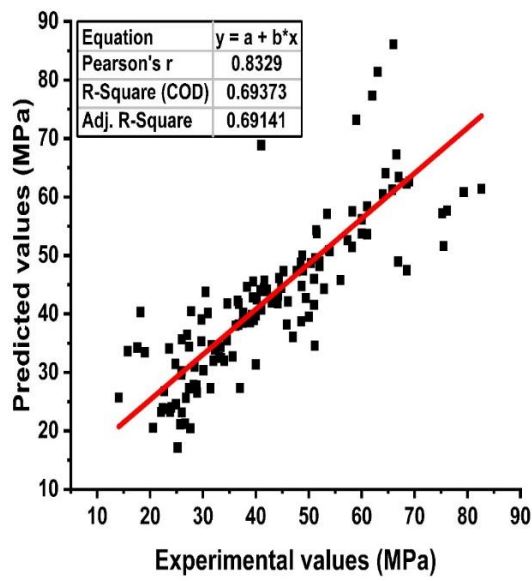
4.5. Sensitivity and Parametric Analysis

Different variables are used to find the CS of RBC. Sensitivity analysis (SA) is used to determine the relative contribution of these variables to the result. SA is carried out mathematically by using the following Equations:

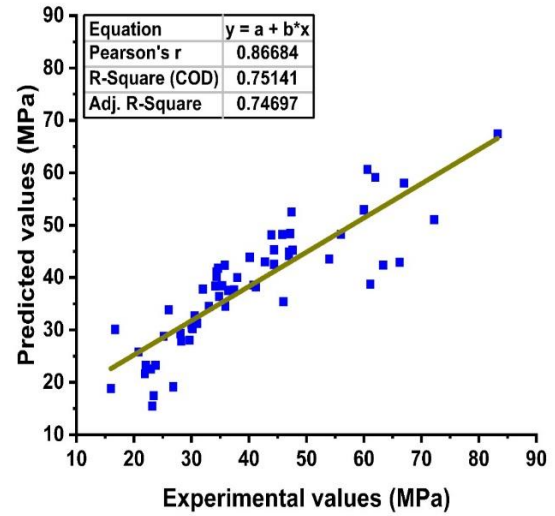
$$N_i = f_{\max}(x_i) - f_{\min}(x_i) \quad (12)$$

$$SA = \frac{N_i}{\sum_{n=1}^j N_j} \quad (13)$$

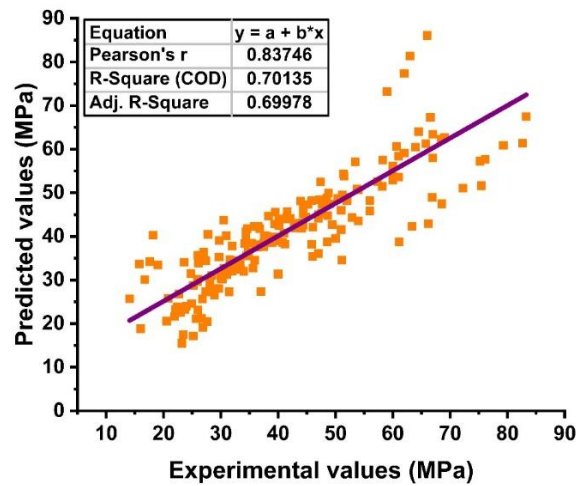
where $f_{\max}(x_i)$ is the maximum, and $f_{\min}(x_i)$ is the minimum output of the predictive models, respectively. Thus, i represents the input domain and other input variables that are kept constant. It is obvious from the graphical representation (shown in Figure 10) that the contribution of different input variables on the CS of RBC is same as that in real life.



(a)

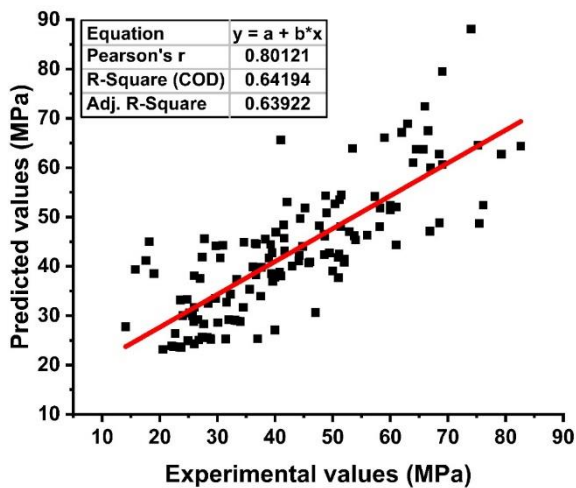


(b)

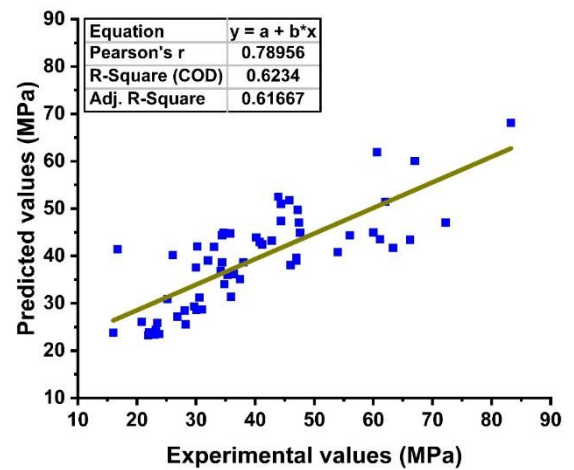


(c)

Figure 8. MNLR (a) training, (b), validation, (c) testing.



(a)



(b)

Figure 9. Cont.

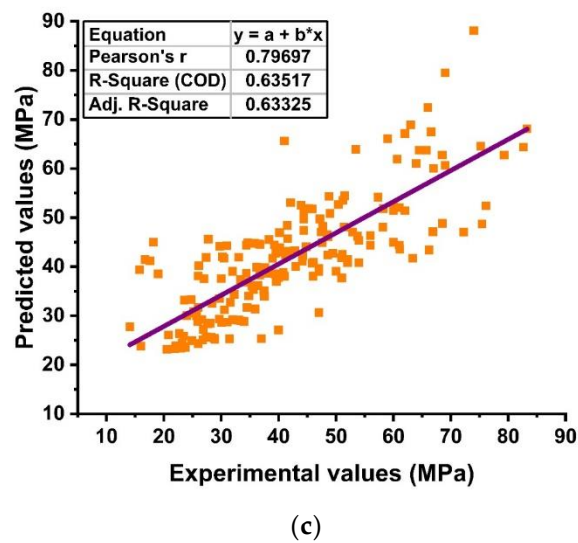


Figure 9. LR (a) training, (b) validation, (c) testing.

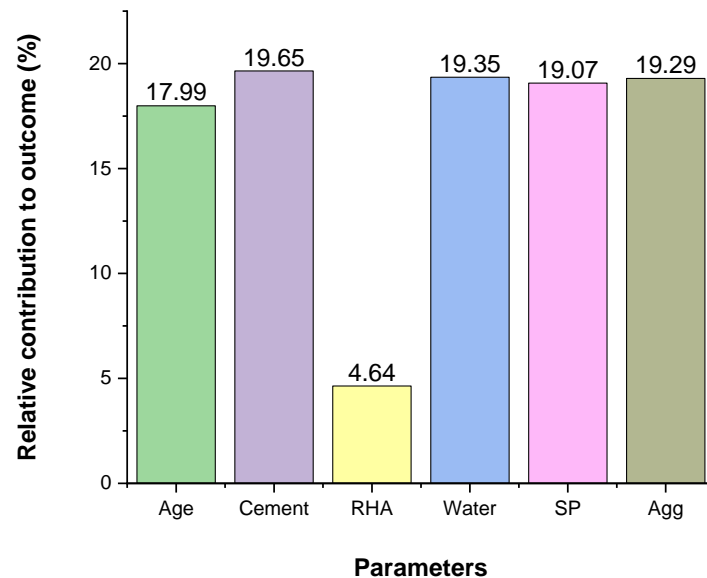


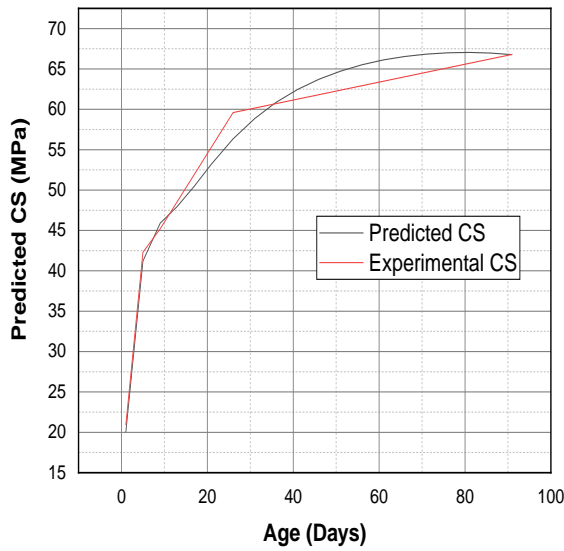
Figure 10. Contribution of inputs to the output.

Along with sensitivity analysis, a parametric analysis (PA) is also carried out. This helps in determining the influence of the input parameters on the output parameter. This shows the trend of CS when all the input variables are kept constant at their mean value except one input. The change in CS is recorded when one input variable is varied from its minimum value to its maximum value. All the results of PA are shown in Figure 11 below.

The sublots in front of each graph in Figure 11 represent the constant parameters of parametric analysis for each input. The literature used for obtaining experimental values includes [12,35–39]. It can be observed from the results that when water is increased from a certain limit, a reduction in CS occurs. This is also obvious from previous studies. De Sensale [39] conducted research in which a water to cement ratio (w/c) of 0.4 gave more CS than w/c of 0.5. RHAP contributes towards the enhancement of strength, but when RHAP is increased by 30 percent, it results in decrease of compressive strength. This is due to the fact that, as discussed in Section 1, RHA contains 90 percent silica. By increasing the RHA percentage, the amount of silica is also increased. This silica remains unreacted by increment of RHA and results in reduced CS of RBC [37].

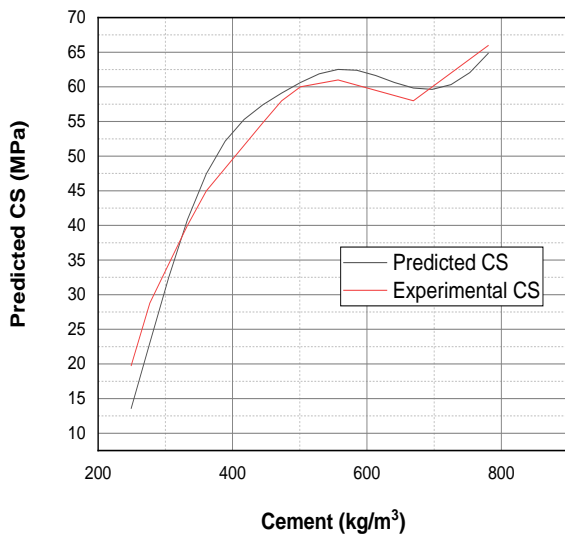
It can be seen from the above results that the regression models did not show satisfactory results as compared to the machine learning processes. This is due to certain

limitations in regression models, such as pre-defined equations that cannot learn the relationship between input variables and the function properly. Whereas, machine learning has efficiently predicted the relationship between input and output variables. The machine learning techniques gave results closer to the experimental values.



(a)

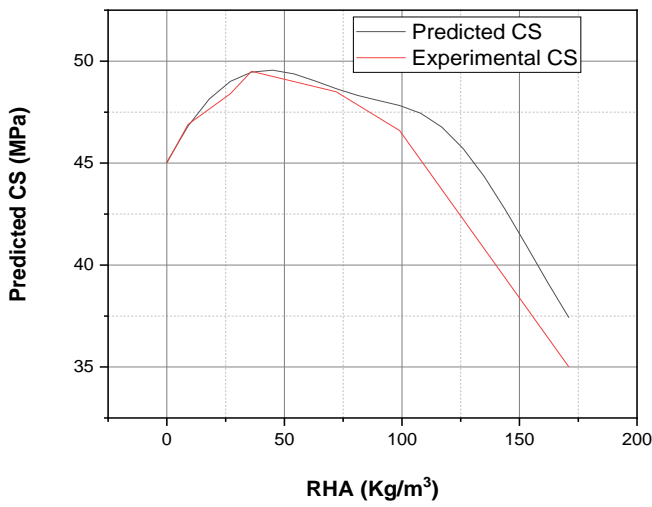
Cement (kg/m ³)	RHA (kg/m ³)	W (kg/m ³)	SP (kg/m ³)	A (kg/m ³)
409	60	192	3	1700



(b)

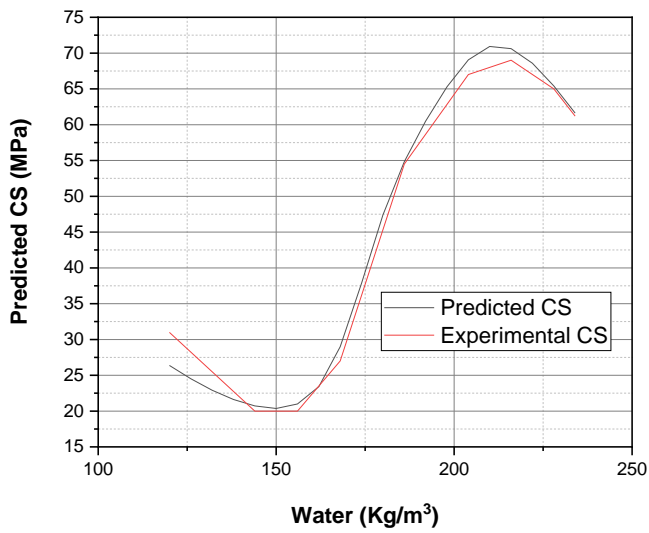
Age (day)	RHA (kg/m ³)	W (kg/m ³)	SP (kg/m ³)	A (kg/m ³)
35	24.9	192	3	1700

Figure 11. Cont.



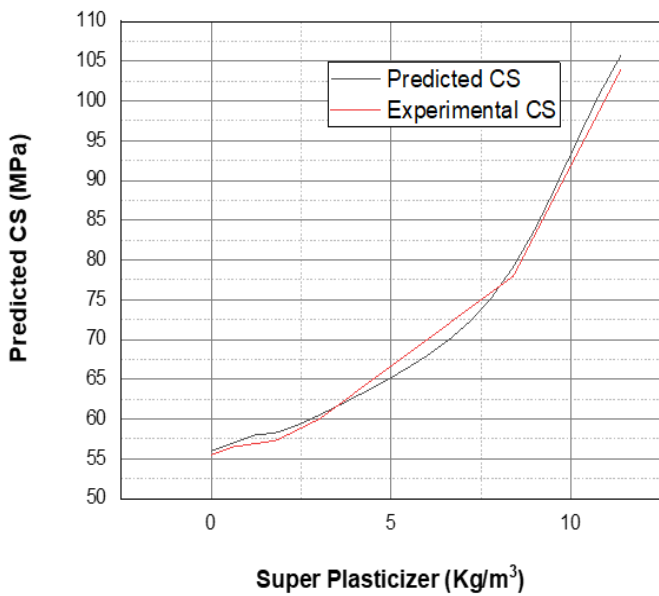
(c)

Age (day)	Cement (kg/m ³)	W (kg/m ³)	SP (kg/m ³)	A (kg/m ³)
35	409	192	3	1700



(d)

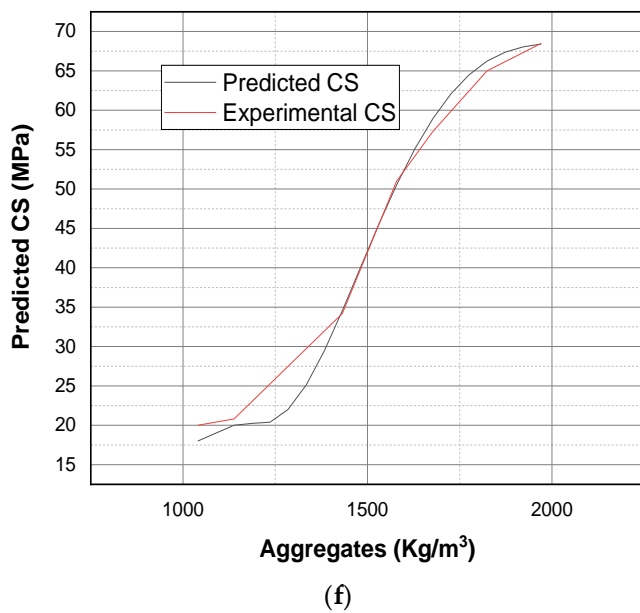
Age (day)	Cement (kg/m ³)	RHA (kg/m ³)	SP (kg/m ³)	A (kg/m ³)
35	409	60	3	1700



(e)

Age (day)	Cement (kg/m ³)	RHA (kg/m ³)	W (kg/m ³)	A (kg/m ³)
35	409	60	192	1700

Figure 11. Cont.



Age (day)	Cement (kg/m ³)	RHA (kg/m ³)	W (kg/m ³)	SP (kg/m ³)
35	409	60	192	3

Figure 11. Parametric analysis of inputs. (a) Age, (b) cement, (c) RHA, (d) water content, (e) superplasticizer, (f) aggregates.

5. Conclusions

Different models for prediction of CS of RBC are developed in this study. The models developed in this study are based on wide range of data which consist of different parameters demonstrated by experimental studies that are available in the literature. The models considered the most influential parameters on CS as inputs. The results obtained in this research are closer to the experimental research. The following conclusions can be drawn from the obtained results:

1. The PA has shown that the input parameters used in this research are effectively utilized by the model to predict the CS. Moreover, the statistical parameter R^2 shows the accuracy of the data used for the training and validation of different models.
2. The R^2 for the predicted strengths of ANN, ANFIS, MNL, and LR is 0.98, 0.89, 0.70, and 0.63, respectively.
3. It is evident by the comparison of ANN and ANFIS with the regression models that both ANN and ANFIS have a high command on prediction of CS of RBC. Therefore, they are suitable for the predesign of RBC.
4. The proposed models can provide the basis for using RBC in different structures rather than discarding it.

Concrete containing RHA has a great potential to replace OPC concrete. It is recommended that extensive research be carried out by including more parameters. These parameters should include temperature, corrosion, and resistance to chlorine and acid attacks. Other advanced programming techniques such as an M5P tree and gene expression programming can be used to make further predictions.

Author Contributions: A.I.: Conceptualization, data analysis, writing original draft and preparation, N.B.K.: Formal analysis and modelling, S.K.-u.-R.: Supervision, review and editing, M.F.J.: Investigation and review, F.A.: Methodology, review and editing, R.A.: Software, validation check and supervision, H.A.: Review, editing and supervision, A.M.: Validation, review, and supervision. All authors have read and agreed to the published version of the manuscript.

Funding: This research received no external funding.

Data Availability Statement: Not applicable.

Acknowledgments: Amir Mosavi would like to thank Alexander von Humboldt Foundation.

Conflicts of Interest: The authors declare no conflict of interest.

Abbreviations

Nomenclature	Definition
AGG	Amount of aggregates
AI	Artificial intelligence
ANFIS	Adaptive neuro-fuzzy inference system
ANN	Artificial neural network
CA	Curing age
CCA	Corn cob ash
CS	Compressive strength
FA	Fly ash
FFBP	Feed forward back propagation
GGBFS	Ground granulated blast furnace slag
GWP	Global warming potential
LR	Linear regression
MLP	Multi layer perceptron
MNLR	Multiple nonlinear regression
OPC	Ordinary Portland cement
OPCP	Amount of OPC
RBC	RHA blended concrete
RH	Rice Husks
RHA	Rice husk ash
RHAP	Amount of RHA
SCBA	Sugarcane baggase ash
SCM	Secondary cementitious material
SLP	Single layer perceptron
SP	Superplasticizer
W	Water used

Appendix A

Table A1. Compressive strength (CS) (MPa) results obtained through different models.

Experimental	ANN Prediction	ANFIS Prediction	LR Prediction	MNLR
18.16	17.91	31.12	45.00	40.31
16.72	12.06	27.21	41.43	30.10
17.6	15.19	31.43	41.21	34.24
15.76	18.26	29.00	39.39	33.65
27.76	30.28	42.86	45.59	40.46
30.24	30.12	43.81	42.02	30.25
27.36	27.30	42.54	41.88	34.41
26.08	29.29	40.42	40.21	33.86
38.32	37.24	33.33	45.51	44.64
33.04	30.89	28.89	41.93	34.44
38.96	36.67	33.62	41.71	38.58
36.16	35.72	31.05	39.89	37.99
14.08	14.95	14.11	27.75	25.72
48.64	50.77	45.60	46.09	44.79
51.12	49.99	45.85	42.52	34.58
48.56	50.10	45.25	42.38	38.75
45.84	48.30	43.04	40.71	38.20
48.48	49.97	37.76	46.52	48.79
40.8	42.73	32.25	42.95	38.59
49.44	51.43	38.02	42.72	42.73
24	23.64	24.81	30.02	24.01

Table A1. Cont.

Experimental	ANN Prediction	ANFIS Prediction	LR Prediction	MNLR
25.2	23.86	25.39	30.85	28.80
26	23.83	27.60	31.67	30.22
28.4	23.95	28.54	32.50	31.01
24.8	24.43	25.31	33.33	31.46
22.08	22.04	22.70	23.90	23.28
23.76	24.07	25.01	23.52	23.27
20.56	20.25	20.97	23.16	20.56
46.08	46.67	35.13	40.90	42.14
66.88	64.77	51.09	47.10	48.94
25.92	23.20	25.88	28.85	29.66
61.12	62.83	49.95	43.53	38.73
66.24	66.69	50.67	43.39	42.90
63.36	60.64	48.28	41.73	42.35
28.24	27.61	26.93	25.55	27.87
28.88	28.21	27.26	25.17	26.58
58.24	60.42	60.99	51.83	57.53
47.68	50.46	49.89	48.25	47.32
58.16	54.92	61.09	48.03	51.46
35.6	36.04	34.11	35.33	32.74
36.4	37.66	34.88	36.16	37.53
39.6	38.16	37.72	36.98	38.95
40	37.39	38.61	37.81	39.75
34.4	35.20	33.55	38.64	40.19
29.68	32.60	29.98	29.33	28.05
33.44	33.46	34.23	28.96	32.49
30.08	29.41	30.17	28.59	30.37
53.76	54.72	56.59	46.21	50.87
76.16	75.21	79.90	52.41	57.68
68.56	67.37	71.43	48.84	47.47
75.44	70.38	79.14	48.70	51.63
32.24	30.73	32.25	34.34	33.92
37.52	32.79	37.51	33.94	38.46
72.24	70.61	75.79	47.04	51.08
41.2	40.88	42.37	42.41	38.23
42.8	43.35	43.43	43.24	43.02
44.8	45.59	46.88	44.06	44.44
47.6	47.49	48.07	44.89	45.24
41.6	49.06	42.34	45.72	45.68
66.56	66.98	66.55	67.50	67.30
53.44	65.68	53.44	63.93	57.09
65.76	66.02	65.76	63.71	61.23
60.64	60.01	60.65	61.89	60.64
34.64	34.06	34.65	44.88	41.78
36.8	36.36	36.85	44.51	41.77
29.76	30.66	29.74	44.14	39.06
44.4	45.77	44.01	51.01	42.51
45.2	45.74	45.49	51.83	47.30
50.4	46.92	49.25	52.66	48.72
51.2	48.40	51.52	53.49	49.52
48.8	49.83	48.52	54.31	49.96
47.2	46.94	47.20	49.75	48.38
83.28	83.60	83.29	68.09	67.45
75.2	75.35	75.20	64.52	57.24
82.64	83.02	82.64	64.38	61.40
79.28	78.48	79.27	62.71	60.85
39.5	39.69	39.50	42.75	45.55
30.5	30.47	30.50	41.75	43.76

Table A1. Cont.

Experimental	ANN Prediction	ANFIS Prediction	LR Prediction	MNLR
29.7	29.35	29.70	33.47	35.31
23.6	23.61	23.60	33.19	34.09
22.7	23.21	22.70	26.39	26.79
20.8	26.18	20.80	26.05	25.81
51.4	50.15	51.40	48.06	54.28
47.4	47.08	47.40	47.06	52.50
40.8	40.61	40.80	38.78	44.04
39.4	40.25	39.40	38.50	42.82
34.5	29.33	34.50	31.70	35.53
35.9	36.13	35.90	31.36	34.54
64.5	64.94	64.50	63.74	64.05
68.5	69.42	68.50	62.74	62.27
51.5	51.89	51.50	54.46	53.81
57.3	57.27	57.30	54.17	52.59
44.4	43.98	44.40	47.38	45.30
52.9	52.55	52.90	47.04	44.31
25.2	26.10	25.23	30.56	17.15
25.68	25.92	25.73	30.00	21.15
26.64	26.24	26.88	29.25	21.23
27.6	26.90	27.46	28.31	20.45
26.88	26.18	26.53	27.20	19.16
23.44	24.15	23.45	25.90	17.47
23.2	21.95	23.16	24.42	15.46
33.36	31.93	33.37	37.39	34.36
34.16	33.71	33.61	36.82	38.37
35.36	36.30	35.56	36.07	38.45
37.44	38.46	36.98	35.14	37.67
34.8	38.45	36.07	34.03	36.38
31.6	37.15	31.50	32.73	34.69
30.56	35.91	30.67	31.25	32.68
39.28	37.51	39.44	44.47	39.86
40.16	39.41	39.95	43.90	43.86
41.68	42.31	42.42	43.15	43.94
44.24	43.81	44.16	42.22	43.16
44.16	42.63	43.10	41.10	41.87
37.6	40.41	37.76	39.81	40.18
36.72	38.56	36.63	38.33	38.17
42.08	43.41	41.98	53.07	44.13
43.92	45.62	43.95	52.50	48.14
45.84	48.62	46.40	51.75	48.21
48.96	48.95	47.45	50.82	47.44
44.4	46.41	45.86	49.70	46.15
41.52	43.25	41.14	48.40	44.46
40.16	40.79	40.18	46.92	42.45
41	40.43	53.59	65.61	68.86
30	30.26	41.92	37.55	31.04
27	28.62	37.95	37.54	36.42
26	26.13	36.87	38.13	35.68
19	19.53	31.29	38.54	33.46
16	15.26	25.75	23.81	18.84
59	52.03	54.44	66.11	73.19
46	39.32	42.89	38.05	35.37
41	38.71	39.35	38.05	40.75
38	37.54	38.27	38.64	40.02
32	32.63	32.88	39.04	37.80
26	25.29	27.13	24.32	23.18
62	60.76	56.13	67.12	77.34
50	47.89	44.83	39.06	39.53
47	48.19	42.14	39.06	44.90

Table A1. Cont.

Experimental	ANN Prediction	ANFIS Prediction	LR Prediction	MNLR
47	47.53	41.06	39.65	44.17
43	43.50	36.06	40.05	41.95
37	35.53	29.91	25.33	27.33
63	64.01	59.09	68.89	81.37
54	52.69	48.22	40.83	43.56
52	53.58	47.03	40.83	48.93
52	52.95	45.93	41.42	48.20
51	48.99	41.63	41.82	45.98
40	41.96	34.77	27.10	31.36
66	67.67	65.01	72.43	86.08
56	56.63	55.01	44.37	48.26
61	58.11	56.80	44.37	53.64
60	58.28	55.69	44.96	52.90
54	55.56	52.77	45.36	50.68
47	47.06	44.48	30.64	36.06
69	70.31	72.59	79.51	91.57
60	61.89	64.09	51.45	53.75
62	63.30	68.19	51.45	59.13
61	63.18	67.77	52.04	58.39
60	60.58	65.74	52.44	56.17
51	51.74	56.18	37.72	41.55
74	72.72	73.15	88.11	95.85
67	67.64	66.03	60.05	58.03
67	68.51	65.54	60.04	63.41
69	67.15	67.40	60.63	62.67
64	63.34	62.65	61.04	60.45
56	54.59	54.77	46.32	45.83
22.08	22.04	22.70	23.90	23.28
22.4	22.26	23.66	23.78	23.84
23.44	23.49	24.42	23.65	23.75
23.76	24.07	25.01	23.52	23.27
22.96	23.29	24.63	23.40	22.55
21.92	21.81	23.13	23.28	21.64
20.56	20.25	20.97	23.16	20.56
27.36	27.33	25.81	25.67	27.31
28.24	27.61	26.93	25.55	27.87
28.8	28.72	27.69	25.42	27.78
31.44	29.08	28.12	25.29	27.30
28.88	28.21	27.26	25.17	26.58
26.8	26.79	25.47	25.05	25.67
24.88	25.41	23.52	24.93	24.59
32	32.36	32.04	29.21	32.01
33.04	32.86	33.46	29.09	32.58
33.44	33.46	34.23	28.96	32.49
34	32.88	34.33	28.83	32.00
31.04	31.26	32.52	28.71	31.28
30.08	29.41	30.17	28.59	30.37
28.08	27.85	28.61	28.47	29.29
34.64	34.06	34.65	44.88	41.78
35.84	36.36	35.81	44.76	42.35
36.56	37.27	36.54	44.64	42.26
36.8	36.36	36.85	44.51	41.77
34.4	34.58	34.26	44.39	41.05
30.96	32.60	31.06	44.26	40.14
29.76	30.66	29.74	44.14	39.06

References

- Chen, C.; Habert, G.; Bouzidi, Y.; Jullien, A. Environmental impact of cement production: Detail of the different processes and cement plant variability evaluation. *J. Clean. Prod.* **2010**, *18*, 478–485. [[CrossRef](#)]

2. Farooq, F.; Ahmed, W.; Akbar, A.; Aslam, F.; Alyousef, R. Predictive modeling for sustainable high-performance concrete from industrial wastes: A comparison and optimization of models using ensemble learners. *J. Clean. Prod.* **2021**, *292*, 126032. [[CrossRef](#)]
3. Mahlia, T.M.I. Emissions from electricity generation in Malaysia. *Renew. Energy* **2002**, *27*, 293–300. [[CrossRef](#)]
4. Akbar, A.; Farooq, F.; Shafique, M.; Aslam, F.; Alyousef, R.; Alabduljabbar, H. Sugarcane bagasse ash-based engineered geopolymer mortar incorporating propylene fibers. *J. Build. Eng.* **2021**, *33*, 101492. [[CrossRef](#)]
5. Mehta, A.; Siddique, R. An overview of geopolymers derived from industrial by-products. *Constr. Build. Mater.* **2016**, *127*, 183–198. [[CrossRef](#)]
6. Tosti, L.; van Zomeren, A.; Pels, J.R.; Damgaard, A.; Comans, R.N.J. Life cycle assessment of the reuse of fly ash from biomass combustion as secondary cementitious material in cement products. *J. Clean. Prod.* **2020**, *245*, 118937. [[CrossRef](#)]
7. Zain, M.F.M.; Islam, M.N.; Mahmud, F.; Jamil, M. Production of rice husk ash for use in concrete as a supplementary cementitious material. *Constr. Build. Mater.* **2011**, *25*, 798–805. [[CrossRef](#)]
8. Adesanya, D.A.; Raheem, A.A. Development of corn cob ash blended cement. *Constr. Build. Mater.* **2009**, *23*, 347–352. [[CrossRef](#)]
9. Crossin, E. The greenhouse gas implications of using ground granulated blast furnace slag as a cement substitute. *J. Clean. Prod.* **2015**, *95*, 101–108. [[CrossRef](#)]
10. Khan, K.; Ullah, M.F.; Shahzada, K.; Amin, M.N.; Bibi, T.; Wahab, N.; Aljaafari, A. Effective use of micro-silica extracted from rice husk ash for the production of high-performance and sustainable cement mortar. *Constr. Build. Mater.* **2020**, *258*, 119589. [[CrossRef](#)]
11. Parveen, S.; Pham, T.M. Enhanced properties of high-silica rice husk ash-based geopolymer paste by incorporating basalt fibers. *Constr. Build. Mater.* **2020**, *245*, 118422. [[CrossRef](#)]
12. Ameri, F.; Shoaie, P.; Bahrami, N.; Vaezi, M.; Ozbakkaloglu, T. Optimum rice husk ash content and bacterial concentration in self-compacting concrete. *Constr. Build. Mater.* **2019**, *222*, 796–813. [[CrossRef](#)]
13. Chao-Lung, H.; Anh-Tuan, B.L.; Chun-Tsun, C. Effect of rice husk ash on the strength and durability characteristics of concrete. *Constr. Build. Mater.* **2011**, *25*, 3768–3772. [[CrossRef](#)]
14. Chindaprasirt, P.; Kanchanda, P.; Sathonsaowaphak, A.; Cao, H.T. Sulfate resistance of blended cements containing fly ash and rice husk ash. *Constr. Build. Mater.* **2007**, *21*, 1356–1361. [[CrossRef](#)]
15. Thomas, B.S. Green concrete partially comprised of rice husk ash as a supplementary cementitious material—A comprehensive review. *Renew. Sustain. Energy Rev.* **2018**, *82*, 3913–3923. [[CrossRef](#)]
16. Rattanachu, P.; Toolkasikorn, P.; Tangchirapat, W.; Chindaprasirt, P.; Jaturapitakkul, C. Performance of recycled aggregate concrete with rice husk ash as cement binder. *Cem. Concr. Compos.* **2020**, *108*, 103533. [[CrossRef](#)]
17. Gursel, A.P.; Maryman, H.; Ostertag, C. A life-cycle approach to environmental, mechanical, and durability properties of ‘green’ concrete mixes with rice husk ash. *J. Clean. Prod.* **2016**, *112*, 823–836. [[CrossRef](#)]
18. Moraes, C.A.M.; Kieling, A.G.; Caetano, M.O.; Gomes, L.P. Life cycle analysis (LCA) for the incorporation of rice husk ash in mortar coating. *Resour. Conserv. Recycl.* **2010**, *54*, 1170–1176. [[CrossRef](#)]
19. Rahman, M.E.; Muntohar, A.S.; Pakrashi, V.; Nagaratnam, B.H.; Sujana, D. Self compacting concrete from uncontrolled burning of rice husk and blended fine aggregate. *Mater. Des.* **2014**, *55*, 410–415. [[CrossRef](#)]
20. Prasara, J.-A.; Grant, T. Comparative life cycle assessment of uses of rice husk for energy purposes. *Int. J. Life Cycle Assess.* **2011**, *16*, 493–502. [[CrossRef](#)]
21. Saraswathy, V.; Song, H.-W. Corrosion performance of rice husk ash blended concrete. *Constr. Build. Mater.* **2007**, *21*, 1779–1784. [[CrossRef](#)]
22. Javed, M.F.; Amin, M.N.; Shah, M.I.; Khan, K.; Iftikhar, B.; Farooq, F.; Aslam, F. Applications of Gene Expression Programming and Regression Techniques for Estimating Compressive Strength of Bagasse Ash based Concrete. *Crystals* **2020**, *10*, 737. [[CrossRef](#)]
23. Ahmad, A.; Farooq, F.; Niewiadomski, P.; Ostrowski, K.; Akbar, A.; Aslam, F.; Alyousef, R. Prediction of Compressive Strength of Fly Ash Based Concrete Using Individual and Ensemble Algorithm. *Materials* **2021**, *14*, 794. [[CrossRef](#)]
24. Hammoudi, A.; Moussaceb, K.; Belebchouche, C.; Dahmoune, F. Comparison of artificial neural network (ANN) and response surface methodology (RSM) prediction in compressive strength of recycled concrete aggregates. *Constr. Build. Mater.* **2019**, *209*, 425–436. [[CrossRef](#)]
25. Jalal, M.; Arabali, P.; Grasley, Z.; Bullard, J.W.; Jalal, H. Behavior assessment, regression analysis and support vector machine (SVM) modeling of waste tire rubberized concrete. *J. Clean. Prod.* **2020**, *273*, 122960. [[CrossRef](#)]
26. Nehdi, Y.D.M.; Khan, A. Neural Network Model for Preformed-Foam Cellular Concrete. *ACI Mater. J.* **2001**, *98*, 5. [[CrossRef](#)]
27. Atici, U. Prediction of the strength of mineral admixture concrete using multivariable regression analysis and an artificial neural network. *Expert Syst. Appl.* **2011**, *38*, 9609–9618. [[CrossRef](#)]
28. Yaseen, Z.M.; Deo, R.C.; Hilal, A.; Abd, A.M.; Bueno, L.C.; Salcedo-Sanz, S.; Nehdi, M.L. Predicting compressive strength of lightweight foamed concrete using extreme learning machine model. *Adv. Eng. Softw.* **2018**, *115*, 112–125. [[CrossRef](#)]
29. Deng, F.; He, Y.; Zhou, S.; Yu, Y.; Cheng, H.; Wu, X. Compressive strength prediction of recycled concrete based on deep learning. *Constr. Build. Mater.* **2018**, *175*, 562–569. [[CrossRef](#)]
30. Bachir, R.; Mohammed, A.M.S.; Habib, T. Using Artificial Neural Networks Approach to Estimate Compressive Strength for Rubberized Concrete. *Period. Polytech. Civ. Eng.* **2018**, *62*, 858–865. [[CrossRef](#)]
31. Altun, F.; Kişi, Ö.; Aydin, K. Predicting the compressive strength of steel fiber added lightweight concrete using neural network. *Comput. Mater. Sci.* **2008**, *42*, 259–265. [[CrossRef](#)]

32. Perera, R.; Barchín, M.; Arteaga, A.; Diego, A.D. Prediction of the ultimate strength of reinforced concrete beams FRP-strengthened in shear using neural networks. *Compos. Part B Eng.* **2010**, *41*, 287–298. [[CrossRef](#)]
33. Tanarslan, H.M.; Secer, M.; Kumanlioglu, A. An approach for estimating the capacity of RC beams strengthened in shear with FRP reinforcements using artificial neural networks. *Constr. Build. Mater.* **2012**, *30*, 556–568. [[CrossRef](#)]
34. Öztaş, A.; Pala, M.; Özbay, E.; Kanca, E.; Caglar, N.; Bhatti, M.A. Predicting the compressive strength and slump of high strength concrete using neural network. *Constr. Build. Mater.* **2006**, *20*, 769–775. [[CrossRef](#)]
35. Bui, D.D.; Hu, J.; Stroeven, P. Particle size effect on the strength of rice husk ash blended gap-graded Portland cement concrete. *Cem. Concr. Compos.* **2005**, *27*, 357–366. [[CrossRef](#)]
36. Ganesan, K.; Rajagopal, K.; Thangavel, K. Rice husk ash blended cement: Assessment of optimal level of replacement for strength and permeability properties of concrete. *Constr. Build. Mater.* **2008**, *22*, 1675–1683. [[CrossRef](#)]
37. Ramezani-pour, A.A.; Mahdikhani, M.; Ahmadibeni, G. The Effect of Rice Husk Ash on Mechanical Properties and Durability of Sustainable Concretes. *Int. J. Civ. Eng.* **2009**, *7*, 83–91. Available online: <https://www.sid.ir/en/journal/ViewPaper.aspx?ID=140499> (accessed on 12 September 2020).
38. Sakr, K. Effects of Silica Fume and Rice Husk Ash on the Properties of Heavy Weight Concrete. *J. Mater. Civ. Eng.* **2006**, *18*, 367–376. [[CrossRef](#)]
39. De Sensale, G.R. Strength development of concrete with rice-husk ash. *Cem. Concr. Compos.* **2006**, *28*, 158–160. [[CrossRef](#)]
40. Golafshani, E.M.; Behnood, A.; Arashpour, M. Predicting the compressive strength of normal and High-Performance Concretes using ANN and ANFIS hybridized with Grey Wolf Optimizer. *Constr. Build. Mater.* **2020**, *232*, 117266. [[CrossRef](#)]
41. Golafshani, E.M.; Behnood, A. Automatic regression methods for formulation of elastic modulus of recycled aggregate concrete. *Appl. Soft Comput.* **2018**, *64*, 377–400. [[CrossRef](#)]
42. Jaafari, A.; Panahi, M.; Pham, B.T.; Shahabi, H.; Rezaie, F.; Lee, S. Meta optimization of an adaptive neuro-fuzzy inference system with grey wolf optimizer and biogeography-based optimization algorithms for spatial prediction of landslide susceptibility. *CATENA* **2019**, *175*, 430–445. [[CrossRef](#)]
43. Gandomi, A.H.; Roke, D.A. Assessment of artificial neural network and genetic programming as predictive tools. *Adv. Eng. Softw.* **2015**, *88*, 63–72. [[CrossRef](#)]
44. Alavi, A.H.; Gandomi, A.H. Prediction of principal ground-motion parameters using a hybrid method coupling artificial neural networks and simulated annealing. *Comput. Struct.* **2011**, *89*, 2176–2194. [[CrossRef](#)]
45. Çaydaş, U.; Haşçalık, A.; Ekici, S. An adaptive neuro-fuzzy inference system (ANFIS) model for wire-EDM. *Expert Syst. Appl.* **2009**, *36 Pt 2*, 6135–6139. [[CrossRef](#)]